Velocity dependence of the cross sections for Penning and associative ionization of H atoms by He(2^1S) metastable atoms

J. Fort, J. J. Laucagne, A. Pesnelle, and G. Watel
Service de Physique Atomique, Centre d'Etudes Nucléaires de Saclay, B. P. No.2-91190 Gif-sur-Yvette, France
(Received 12 January 1976)

The velocity dependence of the Penning and associative ionization cross sections for the He(2^1S) + H interacting system is measured for the relative velocity range 1900–5300 m/sec in a crossed-beam experiment by a time-of-flight technique. We observe that the total ionization cross section decreases monotonically with increasing kinetic energy, and that associative ionization is a minor process, contrary to some theoretical predictions made for the He(2^1S) + H system.

I. INTRODUCTION

The He* + H system is the simplest three-electron diatomic system involving Penning and associative ionization,

$$\mathrm{He}(2^1S, 2^3S) + \mathrm{H} \begin{cases} \xrightarrow{\sigma_{PI}} \mathrm{H}^+ + \mathrm{He} + e, & (1) \\ \xrightarrow{\sigma_{AI}} \mathrm{HeH}^+ + e. & (2) \end{cases}$$

Several calculations of the total ionization and associative ionization cross sections of H atoms by He(2^3S) (Refs. 1–7) and He(2^1S) atoms (Refs. 1–5) have been reported. The results of the different approaches used by these authors have indicated significant discrepancies in the potential curves and the autoionizing widths, especially in the case of the He(2^1S) + H system, and consequently for the ionization cross sections which are deduced from them.

Thus it is of considerable interest to obtain experimental information about this system, especially on the role of the relative kinetic energy of motion of reactants. Until now, the only experimental results on the He(2^1S) + H system concern measurements made without velocity selection,[8,9] i.e., cross sections averaged over the velocity distributions of the colliding atoms.

We have measured the velocity dependence of the Penning and associative ionization cross sections for the He(2^1S) + H interacting system in the thermal energy range 0.015–0.11 eV.

II. EXPERIMENT

A schematic diagram of the apparatus is shown in Fig. 1. The crossed-beam apparatus has been modified from that used in the study of the He* + Ar system,[10] where the same time-of-flight technique was employed.

A. Metastable beam

The metastable He($2^1S + 2^3S$) atoms are produced by electron bombardment of He gas. The source operates with a Ta filament (35 A) producing an electron current of 600 mA with 100 V acceleration potential applied between the filament, and a Mo mesh located about 1 mm from the filament. A Granville Phillips automatic pressure controller and servo-driven valve assembly referenced to a Pirani gauge regulates the He flow in order to obtain a stable pressure optimizing the yield of metastable atoms in the beam; the usual pressure is about 0.15 Torr.

A very thin slit (0.06×2 mm^2) connects the source chamber to the differential pumping chamber in which the pressure rises from 10^{-7} to 8×10^{-6} Torr when the source is on. The beam is shaped into a ribbon by a second slit (0.5×10 mm^2) located 7 cm from the first.

The beam is mechanically chopped by an Al slotted disk located 1 cm from the second slit. The disk (18 cm diam) has five slits: The slit-width was made equal to the effective beamwidth so as to have a triangular gate function. The chopper rotates at 12 000 rpm.

The He(2^1S) component is quenched by optical pumping; the He discharge lamp is a 6-mm-diam helical quartz tube surrounding the beam for a length of 5 cm. It operates continuously at 50 mA and 2000 V at a pressure of 5 Torr, and is cooled by compressed air.

The metastable beam enters a second vacuum chamber through a 1-cm-diam tube 4 cm long and a third slit (3×13 mm^2). The pressure in the second chamber is about 10^{-7} Torr when the metastable-atom source is on. Charged particles are removed from the beam by deflection plates before entering the interaction chamber. The metastable atoms are detected downstream by an electron multiplier (Johnston MM1).

B. H target beam

The interaction chamber is a small rectangular Ti box $28 \times 28 \times 10$ mm^3. Four rectangular slits

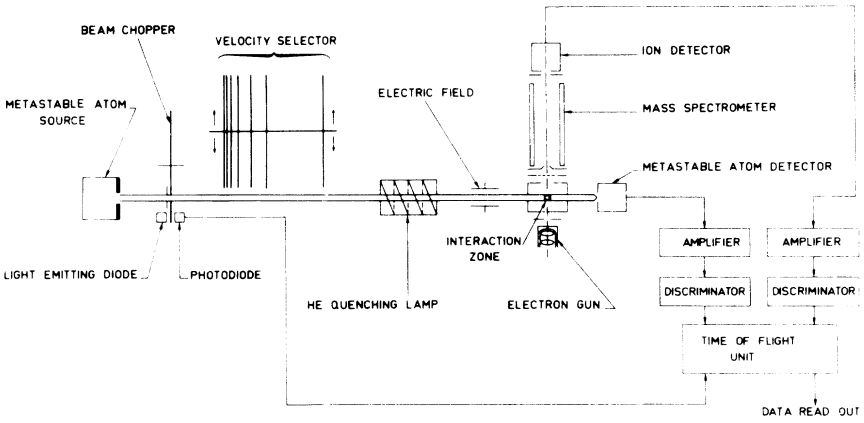

FIG. 1. Schematic diagram of the apparatus. The target H atom beam enters the interaction chamber in a plane perpendicular to the plane of this diagram. For clarity, the distances are not drawn to scale.

6×3 mm^2 in four opposite faces define two mutually perpendicular intersection axes. Before entering the interaction chamber, the H atoms are slowed down by passing them through a 5-cm-long Teflon tube placed in a liquid-nitrogen-cooled stainless-steel block that is located just outside one of the apertures. A radio-frequency discharge is utilized to obtain H atoms. In order to increase the signal-to-noise ratio, the rf discharge is separated from the interaction chamber by about 30 cm, while two 90° bends in the quartz tubing containing the H plasma prohibit the transmission of photons, ions, and excited H_2 molecules. In order to optimize the H atomic concentration, the hydrogen gas pressure in the discharge is chosen to be 0.15 Torr, since we observe that above this pressure the volume recombination increases strongly. Catalytic recombination of atoms on the wall is minimized by carefully cleaning the tubing with orthophosphoric acid.

The ions resulting from He*-H collisions are extracted from the interaction chamber, which is biased at +20 V relative to ground, through a 10.2-mm-diam aperture in the Ti box. This aperture is on an axis centered at the collision zone and perpendicular to the plane of the colliding beams. The ions are focused by an electrostatic lens consisting of the extraction aperture, a 6-mm-diam grid biased at −12 V, and a 4-mm-diam grounded diaphragm; the distance between the elements is 2 mm. The ions are mass selected by a Varian quadrupole mass spectrometer, and are detected by an electron multiplier (Bendix M308) located on the same axis.

An electron gun (indirectly heated cathode) is positioned on the same axis as the quadrupole mass spectrometer but on the opposite side of the interaction chamber. It is used to calibrate the mass scale of the quadrupole analyzer and to choose its resolution.

C. Electronics

All of the time-of-flight (TOF) measurements are performed by counting techniques; the pulses produced by the metastable He atoms on the Johnston MM1 electron multiplier and by the H^+ or HeH^+ ions on the Bendix M308 electron multiplier are processed by fast low-noise amplifier discriminators (Johnston PAD2), and are sent to the input of a TOF unit. The TOF unit is a 256-channel pulse analyzer (TMC CN110) coupled with a TOF logic unit (TMC 211). The channel width can be selected between 0.25 and 64 μsec; for our measurements, a 2-μsec channel width usually gave a satisfactory spectrum. Countdown of the channel scale is triggered by the chopper by use of a light-emitting diode and an optohybrid reader (Centralab CL100 and OH100). The data are automatically punched on a Teletype via the readout unit (TMC 220).

III. RESULTS

A. Data

Since the He($2\,^1S$) component of the metastable beam can be quenched with the helium discharge lamp, the signal corresponding to He($2\,^1S$) atoms is derived by making observations with the lamp on and off.

By varying the extraction lens bias, we have verified that the kinetic energy of the H^+ ions produced by He($2\,^1S$) atoms does not exceed thermal values, unlike the H^+ ions that are produced by He($2\,^3S$) atoms. Therefore only the He($2\,^1S$) + H interaction TOF spectra have been processed, since the extraction lens was especially adjusted to collect thermal ions in this experimental procedure. This observation is consistent with calculations[1,2] which predict a large difference between the two well depths of the He($2\,^1S$) + H and He($2\,^3S$) + H potential curves. The TOF spectra

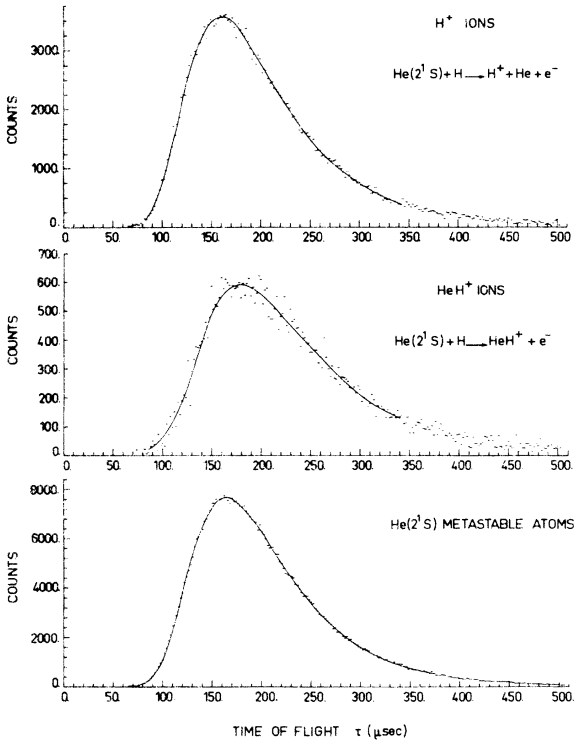

FIG. 2. TOF spectra of H^+ and HeH^+ ions and He ($2\,^1S$) metastable atoms. The channel width is 2 μsec, and the flight path is 46.1 cm for the ion spectra and 50.2 cm for the He($2\,^1S$) spectrum. The zero of the time scale is located in the middle of the chopper gate function. The number of cycles counted is 12×10^6 for ions and 6×10^6 for He($2\,^1S$), with independent counting units.

of the He($2\,^1S$) atoms, and H^+ and HeH^+ ions are shown in Fig. 2.

Photons are emitted by the metastable atom source. They produce H^+ ions in the interaction zone by photoionization. Accumulation of data with no delay gives a H^+ photoion peak in the H^+ TOF spectrum and a photon peak in the He* TOF spectrum, both having the gate-function shape. The photoion peak is delayed by the ion transit time in the mass analyzer. The zero of the time scales is given by the middle of the photon or photoion peak.

Furthermore, we have verified that the extraction and the mass selection of the ions did not modify their TOF spectra by using the TOF technique and a velocity selector for the metastable beam (which has not been used elsewhere in the present work). A triangular He* TOF spectrum is thus obtained, whose base width is related to the resolution of the velocity selector ($R\simeq10\%$). We have observed a similar triangular H^+ TOF spectrum.

Although it has been observed that the H^+ ion production by He($2\,^1S$)-H_2 collisions is negligible compared to the number of H^+ ions produced by He($2\,^1S$)-H collisions, the contribution of the H_2 molecules remaining in the target beam to HeH^+ ion production is not negligible. In order to obtain the HeH^+ TOF spectrum resulting from only He($2\,^1S$)-H collisions, we have subtracted from the HeH^+ TOF spectrum resulting from He*-H, H_2 collisions (hydrogen rf discharge on) the HeH^+ TOF spectrum resulting from He*-H_2 collisions alone (hydrogen rf discharge off), weighted using the dissociation coefficient in the rf discharge.

B. Determination of the effective cross sections from the time-of-flight spectra

The He* atoms are detected by secondary emission. The most general formula for the He* signal is

$$N^*(\tau)\simeq\Delta\tau\int_0^{t_0}A(t)f(L_m/(\tau-t))\times\gamma(L_m/(\tau-t))L_m\,dt/(\tau-t)^2, \tag{3}$$

where $A(t)$ is the chopper gate function whose base width is t_0, f is the velocity distribution of the He* atoms in the beam, γ is the secondary emission coefficient, L_m is the He* flight path, and $\Delta\tau$ is the channel width (as in Ref. 10). Since we have observed that the TOF spectra of He($2\,^1S$) and He($2\,^3S$) atoms are the same, we have assumed that γ is independent of the metastable atom velocity $v=L_m/(\tau-t)$. Formula (3) is then reduced to

$$N^*(\tau)\simeq\Delta\tau\int_0^{t_0}A(t)f(L_m/(\tau-t))L_m\,dt/(\tau-t)^2. \tag{4}$$

The velocity distribution f can be approximated by a modified Maxwellian distribution,

$$f(v)dv\sim v^n e^{-v^2/v_0^2}dv.$$

The parameters n and v_0 (n need not be integral) are determined by fitting formula (4) to the experimental He* TOF spectrum.

The ion signal is given by

$$N^+(\tau)\simeq\Delta\tau\int_0^{t_0}A(t)f(L/(\tau-t))\times\sigma_{\rm eff}(L/(\tau-t))L\,dt/(\tau-t)^2, \tag{5}$$

where L is the distance between the chopper and the interaction chamber and $\sigma_{\rm eff}(v)$ is the effective ionization cross section.

Two methods have been used to derive $\sigma_{\rm eff}$ from the TOF spectra:

(a) The principle of this method is to expand the

cross section in a basis set of q independent functions $p_i(v)$,

$$\sigma_{\text{eff}}(v) = \sum_{i=1}^{q} \alpha_i p_i(v) ,$$

and to estimate the coefficients α_i by performing a least-squares fit of

$$N_q^+(\tau) \simeq \sum_{i=1}^{q} \alpha_i \int_0^{t_0} A(t) f(L/(\tau - t)) \times p_i(L/(\tau - t)) L\, dt/(\tau - t)^2$$

to the experimental ion TOF spectrum.

(b) The second method consists of the deconvolution of the TOF spectra. In the first step, it is necessary to recalculate the He* TOF spectrum for the flight path L instead of L_m. The deconvoluted spectra corresponding to $N^*(\tau)$ [Eq. (4)] and $N^+(\tau)$ [Eq. (5)] are, respectively,

$$n^*(\tau) \sim f(L/\tau) L/\tau^2 ,$$

$$n^+(\tau) \sim f(L/\tau) \sigma_{\text{eff}}(L/\tau) L/\tau^2 .$$

Therefore the effective cross section σ_{eff} is obtained as a function of τ by taking the ratio

$$\sigma_{\text{eff}}(L/\tau) = n^+(\tau)/n^*(\tau) ,$$

and as a function of the He* atom velocity by using the formula $v = L/\tau$.

The deconvolution is achieved by a discrete Fourier transform ($\mathcal{T}$) of the sequence of values representing $N^*(\tau)$ and $N^+(\tau)$ as shown in Fig. 2; n^* and n^+ are then computed by use of the following formulas:

$$n^* = (\mathcal{T})^{-1}[\mathcal{T}(N^*)/\mathcal{T}(A)] ,$$

$$n^+ = (\mathcal{T})^{-1}[\mathcal{T}(N^+)/\mathcal{T}(A)] .$$

The discrete Fourier transforms ($\mathcal{T}$'s) are truncated in order to remove most of the noise while keeping most of the initial signal. The truncating frequency is chosen such that the recalculated convolution products of $n^*(\tau)$ and $n^+(\tau)$ with $A(t)$ fit the experimental TOF spectra $N^*(\tau)$ and $N^+(\tau)$, respectively.

Using the algorithm of Cooley and Tukey[11] to estimate the $\mathcal{T}$, both effective cross sections $\sigma_{\text{eff}}^{\text{AI}}$ and $\sigma_{\text{eff}}^{\text{PI}}$, for associative and Penning ionization, respectively, have required less than 10 sec of IBM 370168 computer time for their computation.[12]

These two methods lead to similar cross sections, with accuracies of the same order of magnitude.

C. Determination of the cross sections σ_{AI} and σ_{PI} and of the ratio $\sigma_{\text{AI}}/(\sigma_{\text{AI}}+\sigma_{\text{PI}})$

The effective cross section $\sigma_{\text{eff}}(v)$ as a function of the He* atom velocity v is defined by

$$\sigma_{\text{eff}}(v) = \int_0^{\infty} v_r\, g(v_t) \sigma(v_r)\, dv_t / v , \tag{6}$$

where $\vec{v}_r = \vec{v} - \vec{v}_t$ is the relative velocity and $g(v_t)$ is the density distribution of the target atom velocities. For orthonormal beams $v_r = (v^2 + v_t^2)^{1/2}$, since in this experiment the H atom velocity v_t is not negligible compared to the He* atom velocity v. If we take the zero of the time scale to be the middle of the gate function, we can use the formula $v = L/\tau$, and then the relative velocity becomes $v_r = (L^2/\tau^2 + v_t^2)^{1/2}$.

From formula (6), we can define an average relative velocity-dependent cross section $\langle \sigma(v_r) \rangle$ by

$$\sigma_{\text{eff}}(v) = \langle \sigma(v_r) \rangle \int_0^{\infty} v_r\, g(v_t)\, dv_t / v = \langle \sigma(v_r) \rangle\, \bar{v}_r / v . \tag{7}$$

The quantity $g(v_t)$ is given by the Maxwell-Boltzmann formula

$$g(v_t) = 4 v_t^2 e^{-v_t^2/v_p^2} / \sqrt{\pi}\, v_p^3 ,$$

where $v_p = (2kT/m_t)^{1/2}$ is the most probable velocity and $\bar{v}_r$ is the average relative velocity,

$$\bar{v}_r = \int_0^{\infty} \left(\frac{L^2}{\tau^2} + v_t^2 \right)^{1/2} g(v_t)\, dv_t . \tag{8}$$

In a first step, assuming that $\sigma(v_r)$ is a v_r^{-n} func-

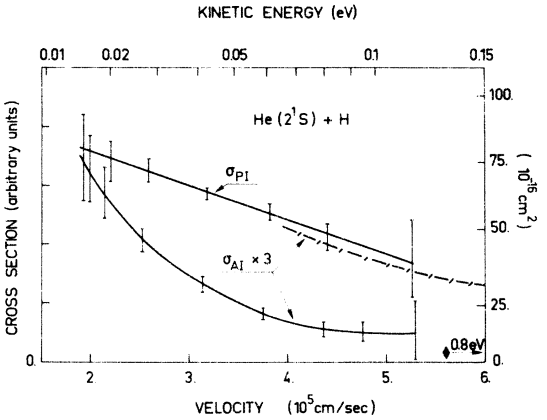

FIG. 3. Associative ionization cross section σ_{AI} and Penning ionization cross section σ_{PI} as a function of relative velocity. ———, present experiment (a smooth curve has been drawn through about 200 points; typical error bars are shown); –/–, theoretical σ_{AI} cross section obtained by Miller and Schaefer (Ref. 1) by counting the resonance states of HeH^+ as dissociated products; ♦, theoretical σ_{AI} cross section (Nakamura, Ref. 3). The experimental results are relative. The absolute scale, shown on the right-hand side of the figure, has been obtained by normalization of the experimental total cross section $\sigma_{\text{TI}} = \sigma_{\text{AI}} + \sigma_{\text{PI}}$ to the value calculated by Cohen and Lane (Ref. 5) at 0.05 eV.

tion, we have verified that the average cross section $\langle\sigma(v_r)\rangle$ as a function of $\bar{v}_r$ is equal to the cross section $\sigma(v_r)$, within the accuracy of the Hermitian quadrature (within <1%), over a range of values of n and T ($0.1 \leq n \leq 0.9$ and $80 \leq T \leq 300$°K) which includes those present in our experiment. Therefore we can obtain the relative velocity-dependent cross section $\sigma(v_r)$ by

$$\sigma(v_r) = v\sigma_{\text{eff}}(v)/\bar{v}_r . \tag{9}$$

In a second step, the cross sections are derived. For each time channel τ of the TOF spectra corresponding to the He* atom velocity v, the average relative velocity $\bar{v}_r$ is calculated with formula (8) and the cross section $\sigma(v_r)$ is derived by formula (9). The velocity dependences of the Penning and associative ionization cross sections are plotted in Fig. 3. They both exhibit a monotonic decrease with increasing velocity.

IV. DISCUSSION

Several calculations of the total ionization cross section σ_{TI} and of the associative ionization cross section σ_{AI} for the He($2\,^1S$) + H interaction have been reported.[1-5] Miller and Schaefer[1] have calculated potential curves for the He($2\,^3S$, $2\,^1S$) + H systems by using a large-scale configuration interaction in which both species exhibit an attractive well. Using a classical orbiting approximation, they have derived σ_{TI} and σ_{AI} for two cases. The first case includes as associated products all of the resonance states of HeH^+ bound in the effective radial potential, while the second case contains only stable molecular ions whose energies are negative with respect to $V^+(\infty)$ [$V^+(R)$ is the $He + H^+$ potential curve]. For our experimental conditions, the resonance states whose energies are positive with respect to $V^+(\infty)$ have enough time to tunnel through the barrier and are detected as dissociated products.

Fujii *et al.*[2] have calculated autoionization widths and potential curves for He($2\,^3S$, $2\,^1S$) + H systems using as a basis product wave functions of the two isolated atoms and a Coulomb wave function for the ejected electron. Their He($2\,^1S$) + H potential curve shows a pure repulsive shape, while the He($2\,^3S$) + H potential curve has an attractive well. Although they obtain a σ_{TI} which increases with increasing energy for the He($2\,^1S$) + H interaction, our experimental σ_{TI} decreases monotonically with increasing energy. Nakamura,[3] using the same widths and potential curves, has extended these calculations to the σ_{AI} associative cross section; the ratio σ_{AI}/σ_{TI} which is then deduced is much higher than the ratio observed experimentally.

Cohen and Lane[4] used the potential curves computed by Miller and Schaefer[1] and the widths calculated by Fujii *et al.*[2] to derive both the $2\,^3S$ and $2\,^1S$ σ_{TI} cross sections. For the $2\,^1S$ system, Cohen and Lane in a later paper[5] combined the $2\,^3S$ width obtained by Miller *et al.*[6] with a large configuration-interaction wave function for the initial He($2\,^1S$)-H resonant state and final He-H^+ state and a Coulomb wave function for the ejected electron. They again obtained a decreasing σ_{TI} cross section with increasing velocity in the range 0.015–0.10 eV, but with absolute values higher than in Ref. 4.

These different theoretical and experimental results are compared in Figs. 3–5. Since our experimental results are relative, the normalization of our cross sections to the most recently published values, i.e., those of Cohen and Lane,[5] has been chosen, although the use of the triplet

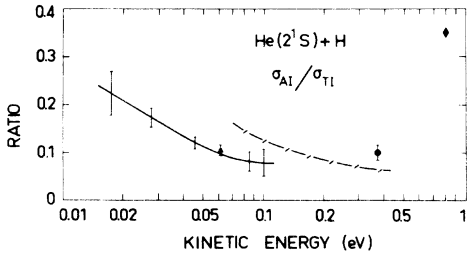

FIG. 4. Ratio σ_{AI}/σ_{TI} as a function of the relative kinetic energy. ———, present experiment (as in Fig. 3); ▲, experimental result, deduced from Hotop *et al.* (Ref. 9); ●, experimental result, Howard *et al.* (Ref. 8); ◆, theoretical result, Nakamura (Ref. 3); –/–, theoretical result, Miller and Schaefer (Ref. 1), obtained by counting the resonance states HeH^+ as dissociated products.

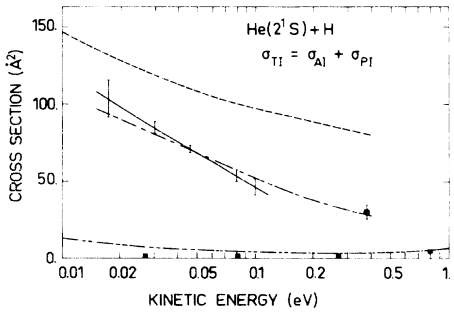

FIG. 5. Total ionization cross section σ_{TI} as a function of relative kinetic energy. ———, present experiment (as in Fig. 3) normalized to the value calculated by Cohen and Lane (Ref. 5) at 0.05 eV; — - —, theoretical curve, Cohen and Lane (Ref. 5); — — —, classical orbiting approximation, Miller and Schaefer (Ref. 1), recalculated by Cohen and Lane (Ref. 5) for small energies; — -- —, theoretical curve, Cohen and Lane (Ref. 4); ■, theoretical result, Fujii *et al.* (Ref. 2); ●, experimental result, Howard *et al.* (Ref. 8).

width by these authors for the He(2 ^{1}S) + H system seems to be a crude approximation.

Looking qualitatively at the cross-section formulas, we see that the cross sections are proportional to the ratio of the width to the relative velocity $\Gamma(R)/v_r$. When the initial He* + H potential curve is attractive, the turning point R_0, and thus the width Γ, remain within a small range of values; consequently the variations of the cross section are mainly governed by v_r, i.e., σ decreases for increasing velocity. But when the initial potential curve is entirely repulsive, R_0 and Γ will vary over a large range of values, and the changes of σ are governed by the two opposite variations of v_r and Γ, i.e., σ increases in the thermal-velocity region but becomes a decreasing function of v_r in the high-velocity region. Thus our experimental results would confirm the existence of an attractive well in the He(2 ^{1}S) + H potential curve, which contradicts the theoretical results of Fujii *et al.*[2]

The values of the σ_{AI}/σ_{TI} ratio do not exceed 24% at 0.015 eV, and are in good agreement with the value deduced from the Penning electron spectrum of Hotop *et al.*[9] at 0.06 eV. This implies that molecular ions are a minor product, which contradicts the results of Miller and Schaefer,[1] whose ratio is roughly 70% higher than our experimental value for the same energy range (0.07–0.11 eV, and Nakamura,[3] whose value (35%) at 0.8 eV is not consistent with our experimental curve. It seems as if more detailed theoretical calculations are necessary to explain the interaction of metastable helium species with hydrogen atoms.

ACKNOWLEDGMENT

The authors wish to express their sincere thanks to Dr. C. Manus for his continuing interest and stimulating discussions.

[1]W. H. Miller and H. F. Schaefer, J. Chem. Phys. 53, 1421 (1970).
[2]H. Fujii, H. Nakamura, and M. Mori, J. Phys. Soc. Jpn. 29, 1030 (1970).
[3]H. Nakamura, J. Phys. Soc. Jpn. 31, 574 (1971).
[4]J. S. Cohen and N. F. Lane, Chem. Phys. Lett. 10, 623 (1971).
[5]J. S. Cohen and N. F. Lane, J. Phys. B 6, L113 (1973).
[6]W. H. Miller, C. A. Slocomb, and H. F. Schaefer, J. Chem. Phys. 56, 1347 (1972).
[7]K. L. Bell, J. Phys. B 3, 1308 (1970).
[8]J. S. Howard, J. P. Riola, R. D. Rundel, and R. F. Stebbings, J. Phys. B 6, L109 (1973).
[9]H. Hotop, E. Illenberger, H. Morgner, and A. Niehaus, Chem. Phys. Lett. 10, 493 (1971); H. Hotop, Radiat. Res. 59, 379 (1974).
[10]A. Pesnelle, A. Hourdin, G. Watel, and C. Manus, J. Phys. B 6, L326 (1973); A. Pesnelle, G. Watel, and C. Manus, J. Chem. Phys. 62, 3590 (1975); J. Fort, J. J. Laucagne, A. Pesnelle, and G. Watel, Chem. Phys. Lett. 37, 60 (1976).
[11]J. W. Cooley and J. W. Tukey, Math. Comput. 19, 297 (1965).
[12]F. Mercier, thesis (University of Paris-Sud, Orsay, 1976)(unpublished).